CREATED USING THE RSC LaTeX PCCP ARTICLE TEMPLATE – SEE www.rsc.org/electronicfiles FOR DETAILS

COMMUNICATION

www. rsc.org/xxxxxx | XXXXXXXX

Engineering Two-Dimensional Hybrid NaCl-Organic Coordinated Nanoarchitectures on Metal Surface

Jérémy Hieulle,[a] David Peyrot,[a] Zhen Jiang,[a] and Fabien Silly*[a]

Received Xth XXXXXXXXXX 20XX, Accepted Xth XXXXXXXXX 20XX
First published on the web Xth XXXXXXXXXX 200X
DOI: 10.1039/b000000x

We selectively engineer three two-dimensional self-assembled hybrid PTCDI-NaCl nanoarchitectures, *i.e.* a flower-structure, a mesh-structure and a chain-structure on Au(111). Scanning tunneling microscopy reveals that NaCl-dimers selectively interact with molecular N-H group. The PTCDI···NaCl-dimer binding appears to be highly directional. Hybrid molecular-ionic self-assembly is a promising alternative to metal-coordinated and multicomponent organic nanostructures to engineer novel nanoarchitectures on surfaces.

Engineering novel atomic and molecular nanostructures on surfaces is a challenge in nanosciences[1]. Perylene diimide derivatives are promising organic building blocks for applications in organic electronics due to their outstanding chemical and thermal stability[2]. These molecules have a non-uniform charge distribution and possess the ability to self-assemble into large two-dimensionnal (2D) hydrogen-bonded nanoarchitectures on flat surfaces[3,4]. Hydrogen-bond (H-bond) is a widely used interaction to govern the formation of organic structures because of the strength, the high selectivity and directionality of this binding[5]. Intense research effort has been focused on tailoring perylene diimide derivative self-assembly to create new nanoarchitectures having different structures and properties[6]. The functionalization of perylene diimide skeleton is used to tune intermolecular interaction to create new arrangements[2,7]. The molecules can also be mixed with complementary organic blocks to create new self-assembled H-bonded nanoarchitectures[8]. Metal-ligand interactions[9,10] are also directional and selective interactions that can be exploited to tailor perylene diimide derivative self-assembly. Jensen *et al.* and Yu *et al.* succeeded in engineering 2D porous structures[11] and 1D single-molecular chains[12] after depositing 3,4,9,10-Perylenetetracarboxylic Diimide (PTCDI, Figure 1a) and nickel adatoms on a gold surface. Despite metal adatoms were hardly distinguishable in the scanning tunneling microscopy (STM) images, the metal-coordinated nanoarchitectures appear to be stabilized by the interaction between the metal adatoms and the molecular oxygen atoms.

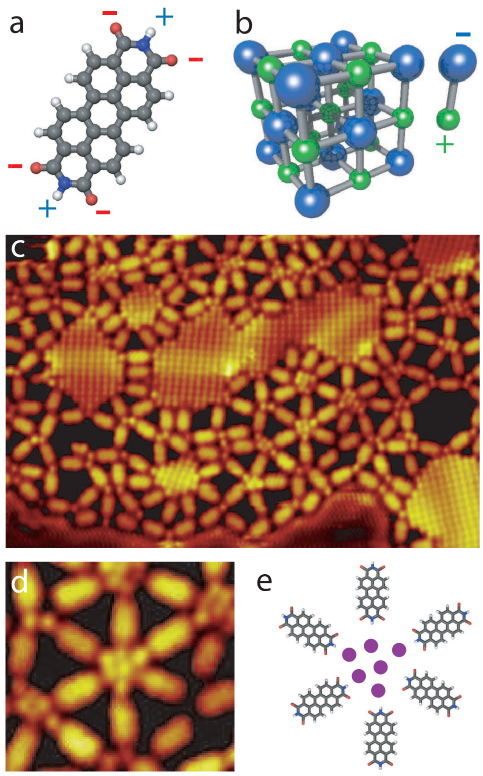

Fig. 1 (a) Charge distribution and scheme of PTCDI. Gray balls are carbon atoms, red balls are oxygen atoms, white balls are hydrogen atoms, and blue balls are nitrogen atoms. (b) NaCl unit cell. Blue balls are chloride and green balls are sodium atoms. (Right) Charge distribution of NaCl dipole. STM image of the PTCDI-NaCl nanoarchitecture after deposition on Au(111)-(22 × $\sqrt{3}$) at room temperature, V_s = 1.2 V, I_t = 0.6 nA; (c) 24×16 nm^2, (d) 5×5 nm^2. (e) Model of NaCl-PTCDI flower observed in (d). NaCl dipoles are represented by purple circles.

H-bonded structures are stabilized by dipole-dipole interactions between molecules whereas metal-coordinated structures are stabilized by metal adatom-molecule electrostatic in-

[a] *CEA, IRAMIS, SPEC, TITANS, CNRS UMR 3680, F-91191 Gif sur Yvette, France. Fax: +33 1 6908 8446; Tel: +33 1 6908 8019; E-mail: fabien.silly@cea.fr*

teractions. Ionic compounds are in contrast stabilized by the electrostatic attraction between negatively-charged anion and positively-charged cation. The strength of this ionic bond can be ten times higher than H-bond interactions [13]. Among ionic materials, sodium chloride (Figure 1b) is an attractive system because it can grow as a multilayer film on numerous metal surfaces when sublimated in vacuum [14]. NaCl can however violently react with polar molecules. H_2O is the archetypal polar molecule, it has a permanent dipole. When H_2O is mixed with NaCl, the positively-charged hydrogen atoms interact with the negatively-charged chloride ions and the negatively-charged oxygen atoms are aligned towards the positively-charged Na ions. This ion-dipole interaction leads to the dissolution of NaCl. Despite the strong NaCl-H_2O interaction, Chen *et al.* showed that a new type of 2D ice structure can grow on NaCl(100) film at low temperature in vacuum [15]. Recent observations in addition revealed that molecule-alkali metal ion interaction can modify 2D supramolecular assembly [16].

Here we investigate the interaction of PTCDI molecules with NaCl on Au(111). Scanning tunneling microscopy (STM) in ultra high vacuum reveals that PTCDI and NaCl self-assemble into three complex 2D hybrid nanoarchitectures depending of surface annealing.

Experiments were performed in a ultrahigh vacuum (UHV) chamber at a pressure of 10^{-8} Pa. The Au(111) surface was sputtered with Ar^{+} ions and then annealed in UHV at 500 °C for 1 hour. PTCDI molecules (Figure 1a) and NaCl (Figure 1b) were evaporated at 250 °C and 390 °C, respectively, on the gold surface kept at room temperature. Cut Pt/Ir tips were used to obtain constant current STM images at room temperature with a bias voltage applied to the sample. STM images were processed and analyzed using the FabViewer application [17].

Figure 1c shows an STM image of the Au(111) surface after the deposition of PTCDI followed by the deposition of NaCl. NaCl flat islands are visible in the image. These islands have almost straight step edges and the angle between the step edges is usually $\sim$90 ° or $\sim$45 °. These NaCl domains appear to be single monolayer islands. The NaCl unit cell with $\sim$4 Å periodicity is resolved in the STM image. This periodicity corresponds to the closest separation of one atomic species in the NaCl(001) surface. The bright spots in the NaCl islands are attributed to Cl^{-} anions [18,19]. Surprisingly the STM images in Figure 1c reveal that PTCDI molecule do not self-assemble into the usual canted-structure [3]. The molecules self-assemble instead into a porous "flower"-network. The flower pattern is presented in the high resolution STM image in Figure 1d. The center of the flower pattern is composed of a small NaCl island. The PTCDI molecules are attached almost perpendicularly to the NaCl island through their short side. This leads to the formation of a molecular flower with an NaCl center and PTCDI molecules as petals.

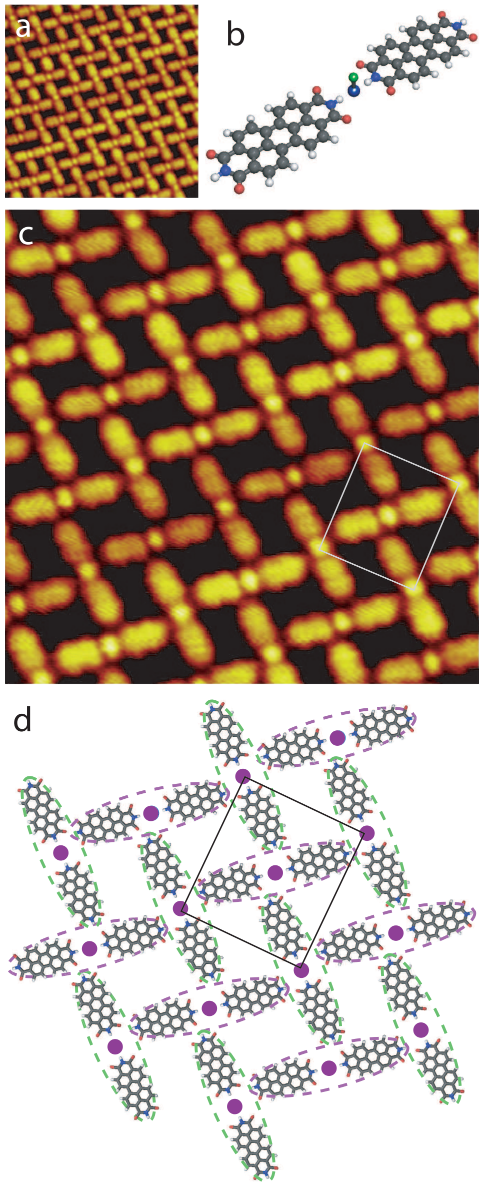

Fig. 2 STM image of the PTCDI-NaCl nanoarchitecture after deposition on Au(111)-(22 × $\sqrt{3}$) at room temperature and post annealing at 100 °C, V_s = 2.0 V, I_t = 0.2 nA; (a) 15×15 nm^2, (c) 10×10 nm^2. (b) Scheme of PTCDI$\cdots$NaCl$\cdots$PTCDI stick (perspective). (d) Model of the Mesh-nanoarchitecture. NaCl dipoles are represented by purple circles.

Temperature is a key parameter that can influence molecular self-assembly [20]. The STM image in Figure 2a reveals that PTCDI molecules and NaCl form a new porous "mesh"-nanoarchitecture after annealing the surface at 100 °C for 40 min. The small NaCl islands are not visible anymore. NaCl appears now as a single round spot (Figure 2c), suggesting it corresponds to a single NaCl dimer. The network unit cell of this porous structure is a rectangle with 2.3 nm and 2.5 nm unit cell constants and an angle of ∼90° between the axes. The model of this porous structure is presented in the Figure 2d. The building block of this nanoarchitecture is a PTCDI···NaCl···PTCDI stick, Figure 2b. The two PTCDI molecules are aligned along their main axis and the NaCl dimer is connected the molecular imide group. This building block is highlighted by dotted ellipses in the model presented in Figure 2d. Neighboring PTCDI···NaCl···PTCDI sticks are almost perpendicular to each other in the "mesh"-nanoarchitecture, Figure 2. The angle between neighboring sticks is in fact ∼80°. Neighboring PTCDI-NaCl sticks appear to be preferentially connected through N-H···O and H···O bonds between PTCDI molecules.

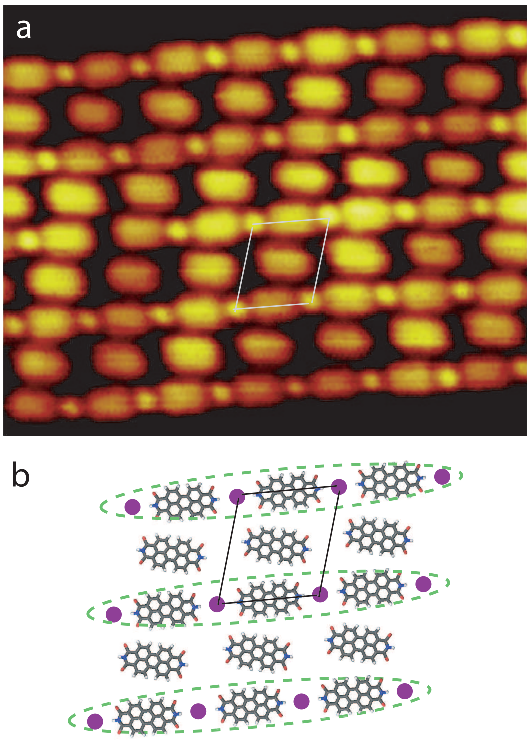

Fig. 3 (a) STM image of the PTCDI-NaCl nanoarchitecture after deposition on Au(111)-(22 × $\sqrt{3}$) at room temperature and post annealing at 150°C, 10×8 nm^2; V_s = 1.9 V, I_t = 0.2 nA. (b) Model of the chain-nanoarchitecture. NaCl dipoles are represented by purple circles.

After annealing the surface at 150°C for 40 min, the STM image shows that PTCDI and NaCl self-assemble into a new epitaxial "chain"-nanoarchitecture (Figure 3a). This structure is composed of parallel PTCDI···NaCl-dimer straight chains (NaCl-dimers appear as a round spots in the STM image). Neighboring PTCDI-NaCl chains are separated by a single PTCDI chain. The molecules are rotated within the PTCDI chains (12°) to promote hydrogen bonding (O···H-C) with the PTCDI molecules of the neighboring PTCDI···NaCl chains. The network unit cell of this porous structure is a parallelogram with 1.5 nm and 1.7 nm unit cell constants and an angle of ∼74° between the axes. The model of this nanoarchitecture is presented in Figure 3b. The parallel PTCDI···NaCl-dimer chains are highlighted by dotted ellipses. NaCl-PTCDI nanoarchitectures are coexisting with PTCDI films (NaCl islands) when PTCDI (NaCl) is in excess, respectively.

STM reveals that the subsequent deposition of NaCl on the Au(111) surface covered with a PTCDI layer leads to the formation of two-dimensional hybrid nanoarchitectures. NaCl essentially forms small islands in the organic layer when deposited on a room temperature surface. NaCl also appears locally as single and paired round spots in the STM images, Figure 1c. There is no evidence of segregation of Na and Cl ions into Na or Cl-rich overlayer in the STM images at room temperature or after annealing. The bright spots localized in the gap between PTCDI molecules (Figures 2, 3) and in the NaCl islands (Figure 1c) have similar contrast in the STM images. These are the reasons why NaCl single bright spots are attributed to single NaCl dimers, with Cl ions adsorbed on the surface. The NaCl dimers appear to break the known PTCDI 2D H-bonded self-assembled structures[3]. The dimers form small 2D clusters in the organic layer at room temperature. The PTCDI molecules are arranged perpendicularly to NaCl islands, *i.e.* molecular imide group is connected to the edge of NaCl clusters. Surface post-annealing at 100°C leads to the dissociation of NaCl islands into NaCl dimers. At high temperature NaCl dimers are trapped between two imide groups of PTCDI. This results into the formation of straight PTCDI···NaCl···PTCDI sticks, Figure 2b. These sticks self-assemble almost perpendicularly into a porous mesh-structure at 100°C. Stick···stick binding appears to be stabilized by double H-bonds (O···H-C) between neighboring PTCDI molecules, Figure 2b. At higher temperature the PTCDI-NaCl mesh-nanoarchitecture collapses to form a new arrangement. PTCDI and NaCl dimers are then arranged sequentially along straight chains. These PTCDI-NaCl chains are separated by single PTCDI chains, Figure 3. The PTCDI molecules are not perpendicular anymore. The chain nanoarchitecture has a higher density (1 mol./128 Å^2) than the mesh-structure (1 mol./144 Å^2).

PTCDI molecules and NaCl strongly interact together to form 2D hybrid nanoarchitectures. Bulk sodium chloride is an ionic crystal with a cubic symmetry. The NaCl structure is composed of dimers consisting of a positively charged sodium ion (Na^+) and a negatively charged chloride ion (Cl^-), Figure 1b. The PTCDI skeleton has a non-uniform internal charge distribution. The oxygen atoms of the imide groups carry a negative partial charge whereas the N-H groups carry a positive partial charge, Figure 1a. The complementary charge distribution of NaCl-dimer and PTCDI appears to be at the origin of the long range self-assembly of these two building blocks. The STM images show that NaCl-dimers and PTCDI molecules are aligned along the main molecular axis, *i.e.* NaCl-dimers are connected to molecular imide groups. We did not observed this interaction when mixing NaCl with PTCDA (3,4,9,10-perylene-tetracarboxylic-dianhydride)[21]. PTCDA shares the same skeleton as PTCDI except that each PTDCI N-H group is replaced by a single oxygen atom in PTCDA. This means that PTCDI N-H group is at the origin of PTCDI···NaCl binding. STM images show that the PTCDI···NaCl interaction is highly directional and selective. Previous calculations suggested that NaCl chlorine atoms appears brighter than Na atoms in the STM images[18,19]. The STM images presented in Figure 1, Figure 2, Figure 3, therefore reveal that the NaCl-PTCDI nanoarchitectures are stabilized by electrostatic interactions between the positively charged PTCDI N-H group and the negatively charged Cl^- ion of NaCl dimer. The Cl^- ion appears to accept the binding of one to two N-H groups. This leads to arrangement of PTCDI and NaCl dimers into straight sticks or chains. The mesh and the chain NaCl-PTCDI nanoarchitectures are both resulting from the assembly of a 2-fold coordination motif (PTCDI···NaCl-dimer···PTCDI, Figure 2b). These nanoarchitectures appear also to be stabilized by H-bonds between neighboring PTCDI molecules. The STM observations show that the NaCl···PTCDI interactions are strong enough to stabilize the formation of porous nanoarchictures at room temperature.

In summary we used scanning tunneling microscopy to investigate the interaction between PTCDI molecules and NaCl in vacuum. STM reveals that PTCDI and NaCl self-assemble on Au(111) and form different hybrid two-dimensional nanoarchitectures depending of surface temperature. These structures are stabilized by H-bonds as well as the selective and directional interaction between NaCl dimers and PTCDI N-H groups. This system is a promising alternative to metal-organic and multicomponent organic structures to engineer novel nanoarchitectures on surfaces.

Acknowledgment: The research leading to these results has received funding from the European Research Council under the European Union's Seventh Framework Programme (FP7/2007-2013) / ERC grant agreement n° 259297.

References

1 (*a*) J. V. Barth, G. Costantini and K. Kern, *Nature*, 2005, **437**, 671–679; (*b*) K. Tahara, J. Adisoejoso, K. Inukai, S. Lei, A. Noguchi, B. Li, W. Vanderlinden, S. D. Feyter and Y. Tobe, *Chem. Commun.*, 2014, **50**, 2831–2833; (*c*) H. Maeda, T. Shirai and S. Uemura, *Chem. Commun.*, 2013, **49**, 5310–5312; (*d*) J. Seibel, L. Zoppi and K.-H. Ernst, *Chem. Commun.*, 2014, **50**, 8751–8753; (*e*) Y. Makoudi, M. Beyer, J. Jeannoutot, F. Picaud, F. Palmino and F. Chérioux, *Chem. Commun.*, 2014, **50**, 5714–5716; (*f*) B. Zha, X. Miao, P. Liu, Y. Wu and W. Deng, *Chem. Commun.*, 2014, **50**, 9003–9006.

2 Y. Avlasevich, C. Li and K. Müllen, *J. Mater. Chem.*, 2010, **20**, 3814–3826.

3 M. Mura, F. Silly, G. A. D. Briggs, M. R. Castell and L. N. Kantorovich, *J. Phys. Chem. C*, 2009, **113**, 21840–21848.

4 (*a*) H. J. Karmel, J. J. Garramone, J. D. Emery, S. Kewalramani, M. J. Bedzyk and M. C. Hersam, *Chem. Commun.*, 2014, **50**, 8852–8855; (*b*) B. Uder, C. Ludwig, J. Petersen, B. Gompf and W. Eisenmenger, *Z. Phys. B*, 1995, **97**, 389–390.

5 (*a*) G. Pawin, K. L. Wong, K.-Y. Kwon and L. Bartels, *Science*, 2006, **313**, 961–962; (*b*) A. R. Ramesh and K. G. Thomas, *Chem. Commun.*, 2010, **46**, 3457; (*c*) O. Ivasenko, J. M. MacLeod, K. Y. Chernichenko, E. S. Balenkova, R. V. Shpanchenko, V. G. Nenajdenko, F. Rosei and D. F. Perepichka, *Chem. Commun.*, 2009, 1192; (*d*) K. Kanazawa, A. Taninaka, H. Huang, M. Nishimura, S. Yoshida, O. Takeuchi and H. Shigekawa, *Chem. Commun.*, 2011, **47**, 11312–11314; (*e*) B. Karamzadeh, T. Eaton, I. Cebula, D. M. Torres, M. Neuburger, M. Mayor and M. Buck, *Chem. Commun.*, 2014, **50**, 14175–14178.

6 J. Hieulle and F. Silly, *J. Mater. Chem. C*, 2013, **1**, 4536–4539.

7 (*a*) S. Yagai, M. Usui, T. Seki, H. Murayama, Y. Kikkawa, S. Uemura, T. Karatsu, A. Kitamura, A. Asano and S. Seki, *J. Am. Chem. Soc.*, 2012, **134**, 7983–7994; (*b*) C. Li and H. Wonneberger, *Adv. Mater.*, 2012, **24**, 613–636.

8 (*a*) R. Madueno, M. T. Räisänen, C. Silien and M. Buck, *Nature*, 2008, **454**, 618–621; (*b*) F. Silly, A. Q. Shaw, M. R. Castell and G. A. D. Briggs, *Chem. Commun.*, 2008, 1907; (*c*) M. E. Canas-Ventura, K. Aït-Mansour, P. Ruffieux, R. Rieger, K. Müllen, H. Brune and R. Fasel, *ACS Nano*, 2011, **5**, 457–469; (*d*) J. A. Theobald, N. S. Oxtoby, M. A. Phillips, N. R. Champness and P. H. Beton, *Nature*, 2003, **424**, 10291031; (*e*) L. M. A. Perdigão, E. W. Perkins, J. Ma, P. A. Staniec, B. L. Rogers, N. R. Champness and P. H. Beton, *J. Phys. Chem. B*, 2006, **110**, 12539–12542.

9 H. Kong, L. Wang, Q. Tan, C. Zhang, Q. Sun and W. Xu, *Chem. Commun.*, 2014, **50**, 3242–3244.

10 J. V. Barth, *Surf. Sci.*, 2009, **603**, 1533–1541.

11 S. Jensen and C. J. Baddeley, *J. Phys. Chem. C*, 2008, **112**, 15439–15448.

12 M. Yu, W. Xu, N. Kalashnyk, Y. Benjalal, S. Nagarajan, F. Masini, E. Laegsgaard, M. Hliwa, X. Bouju, A. Gourdon, C. Joachim, F. Besenbacher and T. R. Linderoth, *Nano Research*, 2012, **5**, 903–916.

13 J. V. Barth, *Annu. Rev. Phys. Chem.*, 2007, **58**, 375–407.

14 (*a*) X. Sun, M. P. Felicissimo, P. Rudolf and F. Silly, *Nanotech.*, 2008, **19**, 495307; (*b*) R. Bennewitz, A. S. Foster, L. N. Kantorovich, M. Bammerlin, C. Loppacher, S. Schär, M. Guggisberg, E. Meyer and A. L. Shluger, *Phys. Rev. B*, 2000, **62**, 2074–2084; (*c*) C. Bombis, F. Ample, J. Mielke, M. Mannsberger, C. J. Villagómez, C. Roth, C. Joachim and L. Grill, *Phys. Rev. Lett.*, 2010, **104**, 185502; (*d*) G. Cabailh, C. R. Henry and C. Barth, *N. J. Phys.*, 2012, **14**, 103037.

15 J. Chen, J. Guo, X. Meng, J. Peng, J. Sheng, L. Xu, Y. Jiang, X.-Z. Li and E.-G. Wang, *Nature Commun.*, 2014, **5**, year.

16 (*a*) T. K. Shimizu, J. Jung, H. Imada and Y. Kim, *Angew. Chem. Int. Ed.*, 2014, **53**, 13729–13733; (*b*) C. Wäckerlin, C. Iacovita, D. Chylarecka, P. Fesser, T. A. Jung and N. Ballav, *Chem. Commun.*, 2011, **47**, 9146–9148; (*c*) D. Skomski, S. Abb and S. L. Tait, *J. Am. Chem. Soc.*, 2012, **134**, 14165–14171.

17 F. Silly, *J. Microsc-Oxford*, 2009, **236**, 211–218.

18 W. Hebenstreit, J. Redinger, Z. Horozova, M. Schmid, R. Podloucky and P. Varga, *Surf. Sci.*, 1999, **424**, L321–L328.

19 K. Glöckler, M. Sokolowski, A. Soukopp and E. Umbach, *Phys. Rev. B*, 1996, **54**, 7705–7708.

20 F. Silly, A. Q. Shaw, K. Porfyrakis, G. A. D. Briggs and M. R. Castell, *Appl. Phys. Lett.*, 2007, **91**, 253109.

21 X. Sun and F. Silly, *Appl. Surf. Sci.*, 2010, **256**, 2228–2231.